Approximate Extraction of Spiralled Horizontal Curves from Satellite Imagery

Haibin Dong[1]; Said M. Easa, M.ASCE[2]; and Jonathan Li[3]

Abstract: Generating road databases from high-resolution satellite imagery is advantageous over traditional methods because of its simplicity and efficiency. Previous research has addressed the extraction of nonspiralled horizontal curves (simple, compound, and reverse curves). All curves were assumed to be circular. This paper presents an approximate method for extracting spiralled horizontal curves. A spiralled horizontal curve consists of a circular curve and a spiral curve at each end that connects the circular curve and the tangent. The spiral curve has a curvature that gradually increases from zero (at the tangent) to the curvature of the circular curve. Because of the symmetry of the spiralled horizontal curve and the semiautomatic nature of the extraction process, the search is three dimensional. Similar to the extraction of nonspiralled horizontal curves, the proposed method performs the search procedures in a smaller area than the image size and achieves faster computations. The method first extracts one side of the road, and a simple procedure for establishing the other side is then applied. The derived curve parameters (circular curve radius, deflection angle, and spiral length) represent useful inputs into a geographic information system database.

DOI: 10.1061/(ASCE)0733-9453(2007)133:1(36)

CE Database subject headings: Satellites; Curvature; Roads; Imaging techniques; Geographic information systems.

Introduction

Remote sensing and geospatial technology offer an innovative tool for improving transportation infrastructure management services, and maintaining accurate inventories and valuations of assets. High-resolution satellite imagery has the potential to facilitate faster, inexpensive techniques to record locations/conditions of assets and to address security concerns related to protecting transportation services. Remote sensing of transportation infrastructure in urban areas is far more challenging than in rural areas, because of the variety of land cover materials with which a given target can be confused. For example, road asphalt appears very much like composite roof shingles in multispectral satellite imagery. Success in road delineation might be improved by using additional information, as provided by the object-oriented image analysis, especially since the spectral separability of different road surface materials is fairly high.

A research project on image-based urban road network extraction has been carried out at the Department of Civil Engineering at Ryerson University (Dong 2003). The specific objectives of this project are to demonstrate how high-resolution commercial satellite images can be utilized to derive the geometric parameters of an urban highway and to assess the utility of the image analysis methods in the context of an urban environment by comparing the performance of the developed methods with existing highway network maps and by showing examples of how the extracted horizontal curves produced by the proposed algorithms could be related to the existing highway curves.

Previous research has addressed the extraction of nonspiralled horizontal curves, including simple, compound, and reverse curves from 1-m spatial resolution IKONOS satellite imagery (Easa et al. 2007). All curves were assumed to be circular. The algorithm presented in the present paper focuses on spiralled horizontal curves. A spiralled horizontal curve consists of a circular curve and a spiral at each end that connects the circular curve and the tangent (Anderson and Mikhail 1998; Kavanagh and Bird 2000; Wolf and Brinker 2000). A spiral is a curve with a uniformly changing radius. Spirals are used in highway alignment to overcome the abrupt change in direction that occurs when the alignment changes from tangent to circular curve, and vice versa. The length of the spiral curve is also used for the transition from normally crowned pavement to fully superelevated pavement. Because of the symmetry of the spiralled horizontal curve and the semiautomatic nature of extraction, the search process is three dimensional.

The purpose of this paper is to explore and test the applicability of an approximate algorithm for extracting spiralled horizontal curves from IKONOS imagery. The following sections describe the approximate algorithm for image-based extraction of spiralled horizontal curves. The extracted results and related discussion are then presented, followed by the conclusions.

[1]Former Graduate Student, Dept. of Civil Engineering, Ryerson Univ., Toronto ON, Canada M5B 2K3.

[2]Professor, Dept. of Civil Engineering, Ryerson Univ., Toronto ON, Canada M5B 2K3.

[3]Associate Professor, Dept. of Civil Engineering, Ryerson Univ., Toronto ON, Canada M5B 2K3.

Note. Discussion open until July 1, 2007. Separate discussions must be submitted for individual papers. To extend the closing date by one month, a written request must be filed with the ASCE Managing Editor. The manuscript for this technical note was submitted for review and possible publication on October 2, 2003; approved on October 21, 2005. This technical note is part of the ***Journal of Surveying Engineering***, Vol. 133, No. 1, February 1, 2007. ©ASCE, ISSN 0733-9453/2007/1-36–40/$25.00.

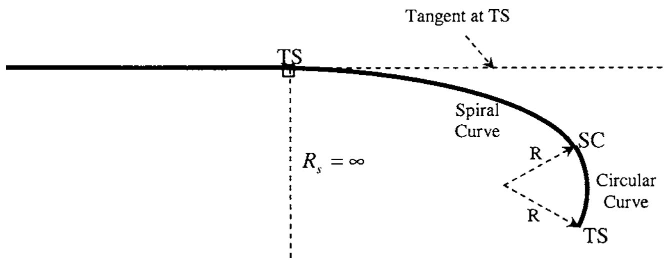

Fig. 1. Characteristics of spiral curve

Proposed Approach

The extraction of the spiralled horizontal curve and associated tangents from the edge image requires some image preprocessing that involves first converting the colored image to a gray image and then generate an edge image from the gray image. The developed algorithm also relies on the Hough transform, a popular algorithm for detecting image features from raster images. Details on image preprocessing and Hough transform are presented elsewhere (Easa et al. 2007). It is useful, however, to describe the Hough transform briefly before presenting the approximate extraction method.

Hough Transform

Generally, the standard Hough transform of a straight line can be represented by (Sonka et al. 1999)

$$\rho = x\cos\alpha + y\sin\alpha \tag{1}$$

where ρ=distance from the origin to the line to be detected; and α=angle between the x axis and a line passing the origin perpendicular to the line to be detected. In an edge image every pixel, whose location is (x,y) and value is not 0, may belong to many lines passing through this pixel. A counter is incremented by 1 for every line passing through this pixel. Thus, after scanning all image pixels, the accumulator contains the number of pixels every line has. A line having pixels greater than a given threshold is a candidate line in this image. The accumulator for saving the counting is a two-dimensional (2D) array $A(\rho,\alpha)$.

The equation of a circle is given by

$$(x-x_0)^2 + (y-y_0)^2 = R^2 \tag{2}$$

where x_0, y_0=coordinates of the center of the circle; and R=radius of the circle. In an edge image, every pixel, whose location is (x,y) and its value is not 0, may belong to many circles whose perimeter passes through the pixel. Similar to line detection, the accumulator array is first initialized, then all pixels are scanned to find the candidate circle. The array is three-dimensional (3D) because the search involves three unknown parameters (x_0, y_0, and R).

Approximate Extraction

A spiral is a curve that commonly connects a tangent to a circular curve. Fig. 1 illustrates how the spiral curve is inserted between tangent and circular curve alignment. It can be seen that at the beginning of the spiral (TS=tangent to spiral) the radius of the spiral is the radius of the tangent line (infinitely large), and that the radius of the spiral curve decreases at a uniform rate until, at the point where the circular curve begins (SC=spiral to curve), the radius of the spiral equals the radius of the circular curve, and

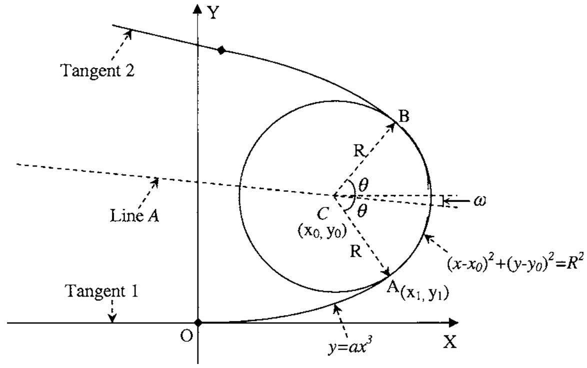

Fig. 2. Symmetrical horizontal curve with spiral approximated by cubic polynomial

vice versa from the beginning of the curve (CS=curve to spiral) to the point where the tangent line starts (ST=spiral to tangent). The spiral provides a smooth transition between the tangent and circular curve, facilitates the development of superelevation, and promotes highway aesthetics (Easa 2002). The spiral may also connect two circular curves with different radii. This paper focuses on spirals that connect two tangents and a circular curve, called here spiralled horizontal curve. This curve is symmetrical which makes the extraction of the curve more efficient.

The curvature (reciprocal of the radius) of the spiral is linearly related to its arc length from TS. For a given point on the spiral i

$$L_i R_i = A \tag{3}$$

where L_i=length of spiral arc from TS to point i; R_i=radius of spiral at Point i; and A=constant. The cubic spiral forms the first-order approximation of the true spiral, and therefore the cubic spiral satisfies the property of Eq. (3) approximately. Let TS be the origin of the coordinate system, where the x axis coincides with the tangent and the y axis is perpendicular to it (Fig. 2). Tangents 1 and 2 intersect at the point of intersection (PI), not shown in Fig. 2. Then, the equation of the cubic spiral and the tangent are given by

$$y = ax^3 \tag{4}$$

$$y = 0 \tag{5}$$

The equation of the circular curve is given by Eq. (2), where R=unknown radius; x_0 and y_0=unknown coordinates of the circular curve center; and a=unknown constant of the cubic spiral. It is possible to detect the spiral in an image and its parameter by modifying a Hough transform. The basic idea is based on finding the parameter of the spiral equation statistically in an image. Since the search of a circle is 3D (x_0, y_0, R), a Hough transform for spiralled horizontal curves would generally involve a 4D search space (x_0, y_0, R, θ), which would be computationally time consuming. However, with the selected coordinate system the search process was reduced to 3D.

The first derivative of the spiral is equal to zero at TS and to that of the circular curve at SC. The first condition is satisfied since the first derivative of Eq. (4) equals 0 at the origin. Regarding the second condition, let the coordinates of Point A be (x_1, y_1). Equating the first derivatives of the circular and spiral curves at Point A gives

J. Surv. Eng., 2007, 133(1): 36-40

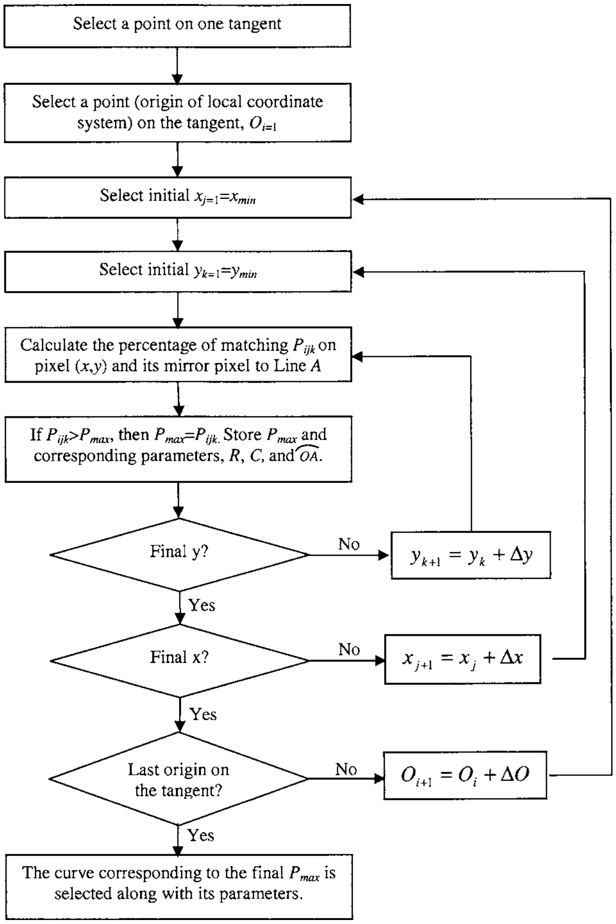

Fig. 3. Flow diagram for approximate extraction of spiralled horizontal curve

$$3ax_1^2=\tan(\theta+\omega) \tag{6}$$

where θ=half the deflection angle of the circular curve; and ω=acute angle between Line A and the x axis (half the curve angle at PI).

The center C of the circular curve must be located on Line A that bisects the curve angle at PI (Fig. 2). Thus, the center C is the intersection point of Line A and the line perpendicular to the tangent at Point A, and θ is the angle between them. The circular curve radius is then calculated as the distance between the center C and Point A. Note that given (x_1,y_1), a can be easily calculated based on Eq. (4). The angle ω can then be calculated based on Eq. (6).

A statistical method, similar to that used in the extraction of circular curves (Easa et al. 2007), was designed for the extraction of the spirals and the adjacent circular arc. For this case, there are three unknowns: one for the origin O and two for Point A (which has two unknowns because it lies within the area enclosed by the x axis, y axis, and the bisector Line A). These unknowns lead to a 3D-search space in the extraction process. Unlike the extraction algorithm for circular curves, a local coordinate system was established for the spiraled horizontal curve, and the origin of this system moves along the tangent line during the search process.

The flow of the proposed extraction algorithm for spiralled horizontal curves is shown in Fig. 3. As noted, there are three unknowns, as previously mentioned, involving the origin O and the coordinates of Point A (x_1,y_1). Thus, the origin of the local coordinate system is dynamic and changes along the tangent in the search procedure. To reduce computation time, the initial origin of the local coordinate system is selected on the tangent whose seed point is closer to the PI. The coordinates (x_1,y_1) give the location of the tested deflection point pixel (Point A), which can be any pixel within the area enclosed by the x axis, y axis, and Line A (Fig. 2). However, in practice the deflection point cannot be very close to the three borders of this area. Therefore, the area for searching the deflection point is deflated by some offsets to the three borders. Arbitrary minimum values of the offsets for x_1 and y_1 were used in the search process, designated as $x_{\min}$ and $y_{\min}$, respectively (Fig. 3). The 3D iterative search determines the best-match combination of the origin O and the coordinates of Point A (x_1,y_1).

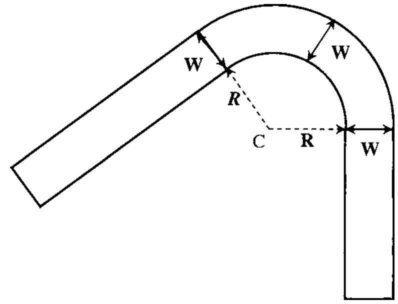

Fig. 4. Extraction of second roadside

Note that the matching scheme considers not only Point A, but also its mirror point on the other side of Line A (Point B). In this way, the search procedures actually find the best fit considering the entire spiralled horizontal curve (the two spirals and the circular curve). This was possible because of the symmetry of the spiralled horizontal curve. The final best-matched combination and the corresponding circular curve radius, circular curve center, and the spiral length OA, and other information are recorded. For this best combination, the length of the extracted spiral is then calculated using a numerical method.

Extracting Second Roadside

Once the edge of one side of a road arc has been found, in terms of the parameters of radius and center position, the other side of the road can be established. The width of a road W is normally constant, especially over the circular curve. Fig. 4 shows the two roadsides of a simple circular curve (the process is similar for spiralled horizontal curves). The inner arc is detected with radius R and center C. It is obvious that the outer curve is an arc with the same center C and a radius equal to $(R+W)$. If the outer roadside is detected first, the inner curve will be an arc with the same center C and a radius $(R-W)$. In both cases, the center of both sides of the road curve is located at C, which is known from the extraction of either arc. What is unknown is only the road width W.

The width of the road is determined by searching for the unknown roadside in the radial direction, either inward or outward, from the circular curve center. To reduce the search space and the possibility of errant detection, the user is required to define which roadside is selected for detection (inner or outer). If it is the inner roadside, the direction of search is outward along the radial direction, and vice versa. The search space is also limited because of the actual road width in the real world. It is assumed that the minimum width of the road is one lane (approximately 4 m wide), and the maximum width is eight lanes (approximately 32 m

J. Surv. Eng., 2007, 133(1): 36-40

Fig. 5. Application 1: Extracting a spiralled horizontal curve (directional ramp)

wide). On the 1 m spatial resolution IKONOS imagery, the search space is converted to pixel units. The conversion is straightforward. For example, the corresponding road width in IKONOS imagery varies from 4 to 32 pixels.

Results and Discussion

The proposed algorithm was applied to extract two freeway interchange ramps that have different characteristics: one is a directional ramp (Fig. 5) and the other is a loop ramp (Fig. 6). The spirals in the image are transition curves connecting a circular curve and tangents at a freeway interchange. The images used in these applications are a subset of the IKONOS imagery, which is a pan-sharpened color IKONOS image with a spatial resolution of

Fig. 6. Application 2: Extracting a spiralled horizontal curve (loop ramp)

Table 1. Parameters of Spiralled Horizontal Curve Extracted in Application 1

Parameter	Values
Parameter of spiral a	0.000020 m^{-2}
Radius of circular curve R	90 m
Half the circular curve angle θ	0.287 rad
Half the curve angle at PI ω	1.62 rad
Spiral deflection angle β	0.169 rad
Coordinates x and y of the origin[a]	253 m, 224 m
Coordinates x and y of Point A	167 m, 185 m
Coordinates x and y of PI	134 m, 353 m
Coordinates of curve center	156 m, 275 m

[a]All coordinates correspond to the image coordinate system whose origin lies at the top-left corner of the image.

1 m. In both applications, the algorithm correctly extracted the spiralled horizontal curve. For example, Fig. 5 shows the extracted simple circular curve (arc A) and the two connecting spirals (Curves B and C). The visual results indicate that the proposed approximate method is satisfactory in extracting symmetrical spiralled horizontal curves. The time required for the computation is similar to that of the 3D search process for reverse and compound curves (Easa et al. 2007).

The extracted variables of the spiralled horizontal curve shown in Fig. 5 are presented in Table 1. The variables include the spiral parameter (a), radius of circular curve (R), circular curve deflection angle (2θ), curve angle at the PI (2ω), spiral deflection angle (β), and (x,y) coordinates of the origin, Point A, PI, and curve center. These variables would represent useful inputs to a geographic information system (GIS) database. Note that the coordinates of the origin and Point A correspond to spiral Curve C in the image.

To confirm the validity of the cubic spiral as a first-order approximation of the original spiral, the properties of the extracted spiral of Fig. 5 were established. Table 2 shows the radius, length, and their product along the extracted cubic spiral. As noted, the spiral length is about 95 m, and the computations were made for 95 points along the spiral. A 1-m increment was used along the x axis and the corresponding y is then calculated from Eq. (4). The spiral is assumed to be linear between consecutive points, and the linear distances are calculated accordingly. For simplicity, the results at five-point increments (in addition to the first and last points) are presented in the table. The bias at the first 36 m of the spiral is less than 1% and is less than 10% up to a spiral length of about 65 m. Only near the last portion of the spiral does the bias increase to larger values. The larger bias results from the fact that the approximate spiral and the circular curve do not have the same second derivatives at SC (or CS), they only have the same first derivative. The bias, as defined by Eq. (3), only indicates the curvature property of the actual spiral. However, a large bias near the connection with the circular curve results in a slight deviation between the locations of the approximate and exact spirals, especially for flat spirals. Such a deviation may not be critical from a practical perspective.

Conclusions and Outlook

An image analysis approach for extracting spiraled horizontal highway curves from high-resolution satellite imagery was presented in this paper. The developed algorithm for extracting spi-

J. Surv. Eng., 2007, 133(1): 36-40

Table 2. Properties of Cubic Spiral Curve Extracted in Application 1

Point number on spiral i	Length on spiral from TS, L_i (m)	Radius of spiral at Point i, R_i (m)	$L_i \times R_i$	Bias (%)
1	1.000	8357.293	8357.293	0.000
5	5.000	1671.464	8357.323	0.000
10	10.000	835.774	8357.772	0.006
15	15.000	557.304	8359.716	0.029
20	20.001	418.224	8364.952	0.092
25	25.003	334.993	8375.997	0.224
30	30.009	279.789	8396.096	0.464
35	35.019	240.706	8429.238	0.861
40	40.037	211.811	8480.177	1.470
45	45.066	189.821	8554.47	2.359
50	50.111	172.786	8658.563	3.605
55	55.179	159.477	8799.829	5.295
60	60.277	149.092	8986.742	7.532
65	65.412	141.091	9229.010	10.431
70	70.595	135.107	9537.799	14.126
75	75.836	130.887	9925.991	18.770
80	80.081	128.666	10303.672	23.290
85	85.462	127.239	10874.055	30.115
90	90.941	127.249	11572.145	38.468
95	95.405	128.273	12237.927	46.434

ralled horizontal curves is based on the first-order approximation of the true spiral. Because of the complexity of the extraction of the unknown parameters of the spiral from imagery, only symmetrical spirals have been considered in this research. In such cases, the search space in an image was reduced to 3D search, which satisfies computational requirements of road extraction from high-resolution satellite imagery. The retrieved parameters include circular curve radius, deflection angle, and spiral length, which can be stored in a GIS database for further uses (such as mapping applications).

The developed computer software was programmed using C^{++}, utilizing much of the computer-vision source code available from Intel, known as OPENCV (Intel 2001). The software implements all the aspects of road extraction, including image pre processing to develop an edge image from a gray image using Canny (1986) method, Hough transform (for lines, circles, and spirals), and the proposed algorithms for extracting simple, reverse, and spiralled horizontal curves.

With the developed algorithms for extracting horizontal curves and associated tangents, it is possible to extract an entire network from an image. The curves can be sequentially extracted one by one until all the road segments of interest have been extracted. The environment may include road and nonroad features. Clearly, human judgement is essential to exclude nonroad, but roadlike features. This is an advantage of the proposed semiautomated extraction methodology. Clearly, this task would be difficult to accomplish using automated extraction methods. Experiments with network extraction in this study have demonstrated that the proposed algorithms operate in an integrated manner to extract both urban networks and freeway interchanges satisfactorily.

This study has shown that high-resolution satellite imagery allows much of the information to be extracted in a GIS environment and the information derived from imagery may add value to the existing attribute-based strategic and tactical highway management practices. Future research may focus on the development of vertical curve extraction algorithms using remote sensing technology. Vertical curves are used in highway vertical alignment to provide a gradual change between two adjacent grade lines. The grade can be derived from digital terrain models (DTM) that can be automatically generated through direct acquisition of georeferenced digital terrain data using airborne laser scanning (or LIDAR) technology. Current studies have shown that LIDAR can provide various surfaces of interest to highway designers, including sloped surfaces in less time and at lower cost than conventional photogrammetric methods. With LIDAR, digital terrain models for an entire corridor can be quickly made, and LIDAR-derived DTMs can be used to refine corridor limits.

Acknowledgments

The research performed is partially funded by Discovery Grant of the National Science and Engineering Council of Canada. The writers wish to thank Anthony Sani of Spatial Geo-link in Toronto for his support with the latest version of ERDAS Imagine. The IKONOS imagery was provided by the Greater Toronto Airports Authority.

References

Anderson, J. M., and Mikhail, E. M. (1998). *Surveying: Theory and practice*. McGraw-Hill, New York.

Canny, J. (1986). “A computational approach to edge detection.” *IEEE Trans. Pattern Anal. Mach. Intell.*, 8(6), 679–698.

Dong, H. (2003). “Semi-automated extraction of urban road networks by geometric analysis of IKONOS imagery.” MASc thesis, Dept. of Civil Engineering, Ryerson Univ., Toronto.

Easa, S. M. (2002). “Geometric design.” in *Civil engineering handbook*, W. F. Chen and J. Y. Liew, eds., Chap. 63, CRC Press, Boca Raton, Fla.

Easa, S. M., Dong, H., and Li, J. (2007). “Use of satellite imagery for establishing road horizontal alignments.” *J. Surv. Eng.*, 133(1), 29–35.

Intel. (2001). *Open source computer vision library: Reference manual.* Internet: www.intel.com

Kavanagh, B. F., and Bird, S. J. (2000). *Surveying—Principles and applications*, Prentice-Hall, Columbus, Ohio.

Sonka, M., Hlavac V., and Boyle, R. (1999). *Image processing, analysis, and machine vision*, PWS Publishing, Toronto.

Wolf, P. R., and Brinker, R. C. (2000). *Elementary surveying*, Harper Collins College Publishers, New York.

J. Surv. Eng., 2007, 133(1): 36-40